Artif Life Robotics (2015) 20:270–275
DOI 10.1007/s10015-015-0223-z

ORIGINAL ARTICLE

Body flexibility effects on foot loading based on quadruped bounding models

Tomoya Kamimura[1] · Yuichi Ambe[1] · Shinya Aoi[2] · Fumitoshi Matsuno[1]

Received: 8 April 2015 / Accepted: 21 July 2015 / Published online: 4 September 2015

Abstract In this paper, we investigate effects of the flexibility of the body on locomotion of a quadruped robot using computer simulation with physical models. So far, many researchers have used legged robots whose bodies consist of one rigid body and examined dynamical properties, such as stability of gaits and energy efficiency. However, from the observation of animals, it has been suggested that flexibility of the body is important for dynamic locomotion. We used two types of simple physical models, with and without a springy joint in their body to evaluate the importance of the body flexibility on the bounding gait, where left and right legs simultaneously kick the ground. Our simulation results show that when we use the same mechanical energy for these two models, the maximum ground reaction force for the model with a body springy joint is smaller than that for the model without a body springy joint (rigid body) even when their locomotion speeds are identical. This suggests that the flexibility of the body can reduce the foot loading of the robot in the bounding gait.

Keywords Quadruped robot · Dynamic walking · Bounding gait · Flexible spine

This work was presented in part at the 20th International Symposium on Artificial Life and Robotics, Beppu, Oita, January 21–23, 2015.

✉ Tomoya Kamimura
kamimura.tomoya.77s@st.kyoto-u.ac.jp

[1] Mechanical Engineering and Science, Graduate School of Engineering, Kyoto University, Room N15, C3 Bldg. d1F, Kyotodaigakukatsura, Nishikyo-ku, Kyoto 615-8540, Japan

[2] Department of Aeronautics and Astronautics, Graduate School of Engineering, Kyoto University, Kyoto, Japan

1 Introduction

Legged animals show diverse locomotor behaviors to adapt to various environments, where they show not only static locomotion, but also dynamic locomotion. For example, they run and jump on cliffs which have limited footholds, and they jump over obstacles while running on grassland. Legged robots also show better mobility than wheeled ones or crawlers [1].

So far, many researchers have used legged robots whose bodies consist of one rigid body to examine dynamical properties during locomotion, such as stability of gaits and energy efficiency. Poulakakis et al. [2, 3] used such legged models in sagittal plane and found stable periodic bounding gaits. Remy et al. [4] developed a passive walking gait model and examined gait stability. Nanua and Waldron [5] developed a quadruped model for trotting, bounding, and galloping gaits and investigated their energy efficiency.

However, from the observation of animals, it has been suggested that flexibility of the body is important for dynamic locomotion. Alexander [6] expressed that mammals use flexibility of the body for fast locomotion. Recently, some researchers developed physical models with flexibility of the body to evaluate the effect on locomotion. Culha and Saranli [7] used an active body joint model with PID control to generate a quadruped bounding gait. Yamasaki et al. [8] used a passive spine joint, which has a rotational spring and damper, and found a periodic bounding gait which achieves a stable limit cycle. Cao and Poulakakis [9, 10] used a passive spine joint model to investigate gait stability and energy efficiency during the bounding gait. However, the effect of the body flexibility on locomotion is still unclear.

Studies of animals also suggest that the ground reaction force is an important factor for dynamic locomotion. For

example, Farlay and Taylor [11] showed that horses change their gaits when the ground reaction force exceeds a threshold. It is important for legged robots to reduce burden, such as the ground reaction force, to avoid damage on legs, the body and actuators. However, any research on the effect of the flexibility of the body on the ground reaction force has not been reported. In this paper, we used two quadruped models with and without a flexible body joint and investigated the effect of flexibility of the body by comparing their results of the ground reaction force in the bounding gait.

2 Models

In this paper, we study on the bounding gait of a quadruped robot, which is modeled as a two legged model in sagittal plane due to the left and right symmetry of the bounding gait. In this section, we explain the bounding gait and two robot models, which we used in this paper.

2.1 Bounding gait

During the bounding gait, left and right legs simultaneously kick the ground and roll and yaw movements of the body are relatively small due to the left and right symmetry of the leg movements. Therefore, we consider the left and right legs as one leg. Although the bounding gait is not necessarily observed as a preferred gait of animals, it is considered as a simple model of galloping gait [1].

The bounding gait has four types of phases for the stance condition, as shown in Fig. 1a. When the fore and hind legs are in the air, we named this phase as Double leg Flight (DF). When only the fore or hind leg is on the ground, we named these phases as Fore leg Stance (FS) or Hind leg Stance (HS), respectively. When both legs are on the ground, we named this phase as Double leg Stance (DS).

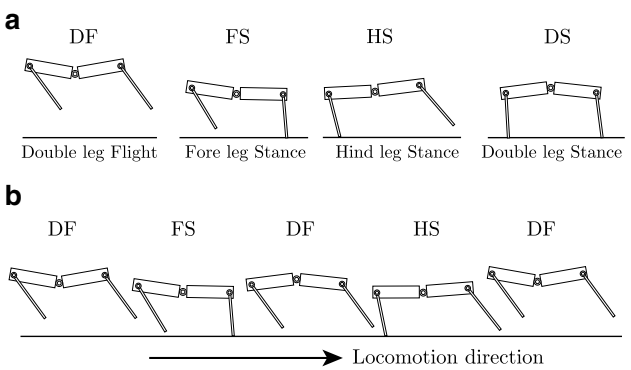

Fig. 1 **a** Four phases for the stance condition, DF, HS, FS, and DS. **b** Sequence of phases in bounding gait

Figure 1b shows the sequence of phases in a periodic bounding gait, which we investigate. This figure starts from an apex height in DF. The fore leg touches the ground, and then lifts off before the hind leg touches the ground. The robot returns to the apex height in DF after the hind leg lifts off the ground. Our simulation results did not obtain the bounding gait which has DS phase.

2.2 Models

In this paper, we used two physical models to investigate the role of flexibility of the body. One model consists of a rigid body and two massless springs (Fig. 2a). The other model is shown in Fig. 2b. The body consists of two rigid bodies, which are connected by a springy joint to simulate the flexibility of the body. Our models are same as those in Poulakakis et al. [3] and Cao and Poulakakis [9]. The model used in [3] is the typical model which has a rigid body. The model used in [9] is one of the minimal models which incorporated the torso bending movement that resembles spinal motions in mammals. Hence we used these two models.

In both models, locomotion direction is the positive direction along the x-axis. g is the gravitational acceleration. The fore and hind springs represent the fore and hind legs, respectively. Both springs have the identical spring constant k_l. l_f^σ and l_h^σ ($\sigma \in \Lambda$, where $\Lambda = \{\mathrm{DF}, \mathrm{FS}, \mathrm{HS}, \mathrm{DS}\}$) are lengths of the fore and hind legs, respectively. γ_f and γ_h are angles of

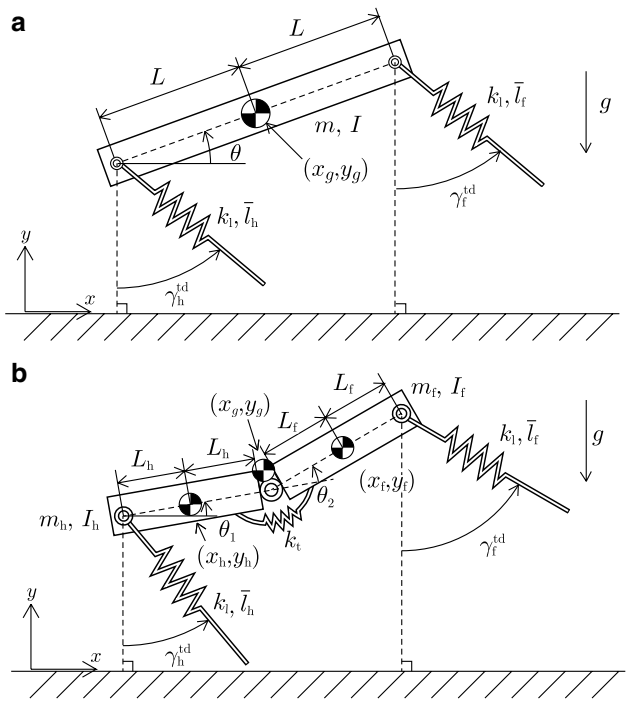

Fig. 2 Quadruped robot models. **a** The rigid body model and **b** the flexible body model

the fore and hind legs relative to the vertical line, respectively. When the springs are in the air, their lengths remain the nominal lengths $\bar{l}_\mathrm{f}$ and $\bar{l}_\mathrm{h}$ and the angles keep the specific values $\gamma_\mathrm{f} = \gamma_\mathrm{f}^\mathrm{td}$ and $\gamma_\mathrm{h} = \gamma_\mathrm{h}^\mathrm{td}$ which correspond to the touchdown angles. When the spring tip reaches the ground, the position of the tip is fixed at the contact point and the tip behaves as a frictionless pin joint. When the spring length returns to the nominal length after the compression, the tip leaves the ground.

In the rigid body model (Fig. 2a), x_g and y_g are the horizontal and vertical positions of the center of mass (COM) of the body, and θ is the pitch angle of the body relative to the horizontal line. m and I are the mass and moment of inertia around the COM, respectively. L is the distance between the COM and the root of the spring. The length of the body is $2L$.

In the flexible body model (Fig. 2b), x_f and y_f are the horizontal and vertical COM positions of the fore body, respectively. x_h and y_h and x_g and y_g are those for the hind body and the whole body. θ_1 is the pitch angle of the hind body relative to the horizontal line. θ_2 is the pitch angle of the fore body relative to the hind body. Masses of the fore and hind bodies are m_f and m_h. Moments of inertia around the COM are I_f and I_h. L_f and L_h are the distances between the fore COM and the root of the fore spring and between the hind COM and the root of the hind spring, respectively. The lengths of the fore and hind bodies are $2L_\mathrm{f}$ and $2L_\mathrm{h}$, respectively. Torsional spring constant of the body joint is k_t. The rotational spring is at the equilibrium position when the fore and hind bodies are in a straight line ($\theta_2 = 0$).

Tables 1 and 2 show the physical parameters of our two models, which were determined based on those in Cao and Poulakakis [9].

Table 1 Physical parameters of the rigid body model

Parameter	Value	Unit
m	20.9	kg
I	2.88	kg m^2
L	0.138	m
$\bar{l}_\mathrm{f}, \bar{l}_\mathrm{h}$	0.360	m
k_l	6340	N/m

Table 2 Physical parameters of the flexible body model

Parameter	Value	Unit
$m_\mathrm{f}, m_\mathrm{h}$	10.4	kg
$I_\mathrm{f}, I_\mathrm{h}$	0.36	kg m^2
$L_\mathrm{f}, L_\mathrm{h}$	0.069	m
$\bar{l}_\mathrm{f}, \bar{l}_\mathrm{h}$	0.360	m
k_l	6340	N/m

3 Equations of motion in two models

Our two models are hybrid system because the governing equation switches depending on the stance condition. In this section, we derive the equations of motion of these models.

3.1 Energy of the rigid body model

Five variables $[x_g\ y_g\ \theta\ l_\mathrm{f}^\sigma\ l_\mathrm{h}^\sigma]\,(\sigma \in \Lambda)$ determine the dynamics of the rigid body model as shown in Fig. 2a. Because the legs have no mass, when the legs are in the air, they have no effect on the body dynamics and $l_i^\sigma = \bar{l}_i$ $(i = \mathrm{f}, \mathrm{h})$ is satisfied. When the legs are on the ground, l_i^σ is described by three variables $[x_g\ y_g\ \theta]$ and the toe positions of the contact legs. We describe the equations of motion of this model using three variables: $\boldsymbol{q}_\mathrm{r} = [x_g\ y_g\ \theta]^\mathrm{T}$. We define T^r as kinetic energy and V_σ^r as potential energy for each phases, which are given by

$$T^\mathrm{r} = \frac{1}{2}m(\dot{x}_g^2 + \dot{y}_g^2) + \frac{1}{2}I\dot{\theta}^2, \tag{1}$$

$$V_\sigma^\mathrm{r} = mgy_g + \frac{1}{2}\left\{k_\mathrm{f}(l_\mathrm{f}^\sigma - \bar{l}_\mathrm{f})^2 + k_\mathrm{h}(l_\mathrm{h}^\sigma - \bar{l}_\mathrm{h})^2\right\}, \tag{2}$$

where l_f^σ and l_h^σ depend on the stance condition as follows:

$$l_\mathrm{f}^\sigma = \begin{cases} \bar{l}_\mathrm{f}, & (\sigma \in \{\mathrm{DF}, \mathrm{HS}\}) \\ \sqrt{A^2 + C^2}, & (\sigma \in \{\mathrm{FS}, \mathrm{DS}\}) \end{cases}$$

$$l_\mathrm{h}^\sigma = \begin{cases} \bar{l}_\mathrm{h}, & (\sigma \in \{\mathrm{DF}, \mathrm{FS}\}) \\ \sqrt{B^2 + D^2}, & (\sigma \in \{\mathrm{HS}, \mathrm{DS}\}) \end{cases}$$

$$A = x_\mathrm{f}^\mathrm{toe} - L\cos\theta - x_g,$$
$$B = x_\mathrm{h}^\mathrm{toe} + L\cos\theta - x_g,$$
$$C = y_g + L\sin\theta,$$
$$D = y_g - L\sin\theta.$$

$x_\mathrm{f}^\mathrm{toe}$ and $x_\mathrm{h}^\mathrm{toe}$ are the x-axis positions of the fore and hind toes on the ground.

3.2 Energy of the flexible body model

Six variables $[x_g\ y_g\ \theta_1\ \theta_2\ l_\mathrm{f}^\sigma\ l_\mathrm{h}^\sigma]$ $(\sigma \in \Lambda)$ determine the dynamics of the flexible body model as shown in Fig. 2b. Similarly to the previous model in Sect. 3.1, we describe the equations of motion of this model by four variables: $\boldsymbol{q}_\mathrm{s} = [x_g\ y_g\ \theta_1\ \theta_2]^\mathrm{T}$. We define T^s as kinetic energy and V_σ^s as potential energy for each phases as follows:

$$\begin{aligned} T^\mathrm{s} = {} & \frac{1}{2}\left\{m_\mathrm{f}(\dot{x}_\mathrm{f}^2 + \dot{y}_\mathrm{f}^2) + m_\mathrm{h}(\dot{x}_\mathrm{h}^2 + \dot{y}_\mathrm{h}^2)\right\} \\ & + \frac{1}{2}\{I_\mathrm{f}(\dot{\theta}_1^2 + \dot{\theta}_2^2) + I_\mathrm{h}\dot{\theta}_1^2\}, \end{aligned} \tag{3}$$

$$V_\sigma^{\mathrm{s}} = (m_{\mathrm{f}} y_{\mathrm{f}} + m_{\mathrm{h}} y_{\mathrm{h}})g + \frac{1}{2}\left\{k_{\mathrm{t}}\theta_2^2 + k_{\mathrm{f}}(l_{\mathrm{f}}^\sigma - \bar{l}_{\mathrm{f}})^2 + k_{\mathrm{h}}(l_{\mathrm{h}}^\sigma - \bar{l}_{\mathrm{h}})^2\right\}, \quad (4)$$

where $(x_{\mathrm{f}}, y_{\mathrm{f}})$ and $(x_{\mathrm{h}}, y_{\mathrm{h}})$ are the COM positions of the fore and hind bodies, respectively. They are given by

$$x_{\mathrm{f}} = x_g + \frac{m_{\mathrm{h}}}{m_{\mathrm{f}} + m_{\mathrm{h}}}\{l_{\mathrm{f}}^\sigma \cos(\theta_1 + \theta_2) + l_{\mathrm{h}}^\sigma \cos\theta_1\},$$
$$y_{\mathrm{f}} = y_g + \frac{m_{\mathrm{h}}}{m_{\mathrm{f}} + m_{\mathrm{h}}}\{l_{\mathrm{f}}^\sigma \sin(\theta_1 + \theta_2) + l_{\mathrm{h}}^\sigma \sin\theta_1\},$$
$$x_{\mathrm{h}} = x_g + \frac{m_{\mathrm{f}}}{m_{\mathrm{f}} + m_{\mathrm{h}}}\{l_{\mathrm{f}}^\sigma \cos(\theta_1 + \theta_2) - l_{\mathrm{h}}^\sigma \cos\theta_1\},$$
$$y_{\mathrm{h}} = y_g + \frac{m_{\mathrm{f}}}{m_{\mathrm{f}} + m_{\mathrm{h}}}\{l_{\mathrm{f}}^\sigma \sin(\theta_1 + \theta_2) - l_{\mathrm{h}}^\sigma \sin\theta_1\},$$

where l_{h}^σ and l_{f}^σ depend on the stance condition as follows:

$$l_{\mathrm{f}}^\sigma = \begin{cases} \bar{l}_{\mathrm{f}}, & (\sigma \in \{\mathrm{DF}, \mathrm{HS}\}) \\ \sqrt{E^2 + G^2}, & (\sigma \in \{\mathrm{FS}, \mathrm{DS}\}) \end{cases}$$
$$l_{\mathrm{h}}^\sigma = \begin{cases} \bar{l}_{\mathrm{h}}, & (\sigma \in \{\mathrm{DF}, \mathrm{FS}\}) \\ \sqrt{F^2 + H^2}, & (\sigma \in \{\mathrm{HS}, \mathrm{DS}\}) \end{cases}$$
$$E = x_{\mathrm{f}}^{\mathrm{toe}} - L_{\mathrm{f}} \cos\theta_1 - x_{\mathrm{f}},$$
$$F = x_{\mathrm{h}}^{\mathrm{toe}} + L_{\mathrm{h}} \cos\theta_1 - x_{\mathrm{h}},$$
$$G = y_{\mathrm{f}} + L_{\mathrm{f}} \sin(\theta_1 + \theta_2),$$
$$H = y_{\mathrm{h}} - L_{\mathrm{h}} \sin(\theta_1 + \theta_2).$$

$x_{\mathrm{f}}^{\mathrm{toe}}$ and $x_{\mathrm{h}}^{\mathrm{toe}}$ are x-axis positions of the fore and hind toes on the ground.

3.3 Equations of motion

Let us define Lagrangian

$$L_\sigma^\alpha = T^\alpha - V_\sigma^\alpha, \quad (\sigma \in \Lambda,\ \alpha \in \Gamma) \quad (5)$$

where $\Gamma = \{\mathrm{r}, \mathrm{s}\}$. From Lagrangian equation, the equations of motion of the two models are given by

$$\frac{d}{dt}\left(\frac{\partial L_\sigma^\alpha}{\partial \dot{\boldsymbol{q}}_\alpha}\right) - \frac{\partial L_\sigma^\alpha}{\partial \boldsymbol{q}_\alpha} = 0, \quad (\sigma \in \Lambda,\ \alpha \in \Gamma). \quad (6)$$

4 Simulation

To find a periodic bounding gait, we define the Poincaré section at $\dot{y}_g = 0$ and $\sigma = \mathrm{DF}$. We assume that both legs have to experience the stance phase at least once before the intersection with the Poincaré section so that the solution explains a gait. The state variables at the Poincaré section can be represented by $\boldsymbol{z}_{\mathrm{r}} = [y_g\ \theta\ \dot{x}_g\ \dot{\theta}]^{\mathrm{T}}$ for the rigid body model and by $\boldsymbol{z}_{\mathrm{s}} = [y_g\ \theta_1\ \theta_2\ \dot{x}_g\ \dot{\theta}_1\ \dot{\theta}_2]^{\mathrm{T}}$ for the flexible body model, where we neglect x_g because the horizontal position monotonically increases during locomotion and is not periodic. The Poincaré map P is denoted as follows:

$$\boldsymbol{z}_\alpha^{n+1} = P(\boldsymbol{z}_\alpha^n, \boldsymbol{u}_\alpha), \quad (\alpha \in \Gamma) \quad (7)$$

where $\boldsymbol{z}_\alpha^n$ is the value of $\boldsymbol{z}_\alpha$ at the nth intersection with the Poincaré section and $\boldsymbol{u}_\alpha$ is the parameter set ($\boldsymbol{u}_{\mathrm{r}} = [\gamma_{\mathrm{f}}^{\mathrm{td}}\ \gamma_{\mathrm{h}}^{\mathrm{td}}]^{\mathrm{T}}$ for the rigid body model and $\boldsymbol{u}_{\mathrm{s}} = [k_{\mathrm{t}}\ \gamma_{\mathrm{f}}^{\mathrm{td}}\ \gamma_{\mathrm{h}}^{\mathrm{td}}]^{\mathrm{T}}$ for the flexible body model).

For a periodic gait, $\boldsymbol{z}_\alpha^* = P(\boldsymbol{z}_\alpha^*, \boldsymbol{u}_\alpha^*)$ is satisfied, where $\boldsymbol{z}_\alpha^*$ is a fixed point on the Poincaré section. We used $y_g^* = 0.32$ m for both our models from the results of Cao and Poulakakis [9] and used $E_{\mathrm{total}}^\alpha = T^\alpha + V_\sigma^\alpha = 290$ J, $\alpha \in \Gamma$ for all σ. In addition, we used symmetric conditions for periodic solution $\gamma_{\mathrm{f}}^{\mathrm{lo}} = -\gamma_{\mathrm{h}}^{\mathrm{td}}$ and $\gamma_{\mathrm{h}}^{\mathrm{lo}} = -\gamma_{\mathrm{f}}^{\mathrm{td}}$, where $\gamma_{\mathrm{f}}^{\mathrm{lo}}$ and $\gamma_{\mathrm{h}}^{\mathrm{lo}}$ are the lift-off angles of the fore leg and the hind leg, respectively [1, 3]. Under these conditions, we searched for the states $\boldsymbol{z}_\alpha^*$ and parameter sets $\boldsymbol{u}_\alpha^*$ that satisfy $\boldsymbol{z}_\alpha^* = P(\boldsymbol{z}_\alpha^*, \boldsymbol{u}_\alpha^*)$. We used the function `fsolve` on MATLAB to search a fixed point for a periodic bounding gait.

5 Results

We found periodic bounding gaits for our two models that have various average speeds. Because the touch down and liftoff occur at the nominal length and the body joint has no dissipation, both physical systems are energy conservative. Thus it is difficult to introduce energy efficiency as a criterion of the effect of the body flexibility based on the derived models. We consider ground reaction force as a criterion. Figure 3 shows the results of the time profiles of y_g and ground reaction force (GRF) for one gait cycle of the periodic gaits, whose average speeds $\bar{v}$ are 4.0, 4.25, and 4.5 m/s, for the rigid body model (Fig. 3a) and the flexible body models with $k_{\mathrm{t}} = 200$ (Fig. 3b) and 260 Nm/rad (Fig. 3c). Ground reaction forces are identical between the fore and hind legs due to the symmetric condition of the gait.

Figure 4 shows the maximum GRFs for each average speed $\bar{v}$ for the rigid body model and the flexible body models with $k_{\mathrm{t}} = 200, 220, 240$, and 260 Nm/rad. This shows that the maximum GRFs for the flexible body model are smaller than that of the rigid body model in all range of locomotion speeds where we found solutions. In addition, the maximum GRFs decrease as k_{t} increases. However, the maximum GRFs did not converge to those of the rigid body model as k_{t} increasing.

Here, we discuss the reason why the GRFs of the flexible body model are less than those of the rigid body model. Figure 3 shows that the amplitude of vertical COM movement y_g decreases for a flexible body joint. This reduces the amount of the compression of leg springs, and then decreases the ground reaction forces. To clearly show this, we show the time profile of energy ratio for one gait cycle at $\bar{v} = 4.5$ m/s in Fig. 5. Figure 5a, b shows the results of

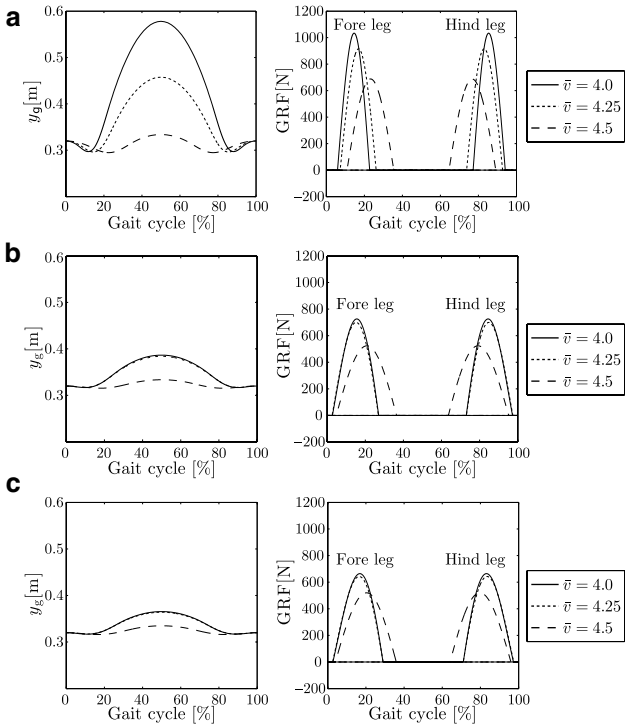

Fig. 3 Simulation results of time profile of y_g and ground reaction forces. $\bar{v}$ is the obtained average speed. **a** The rigid body model, **b** the flexible body model with $k_t = 200$ Nm/rad, and **c** the flexible body model with $k_t = 260$ Nm/rad

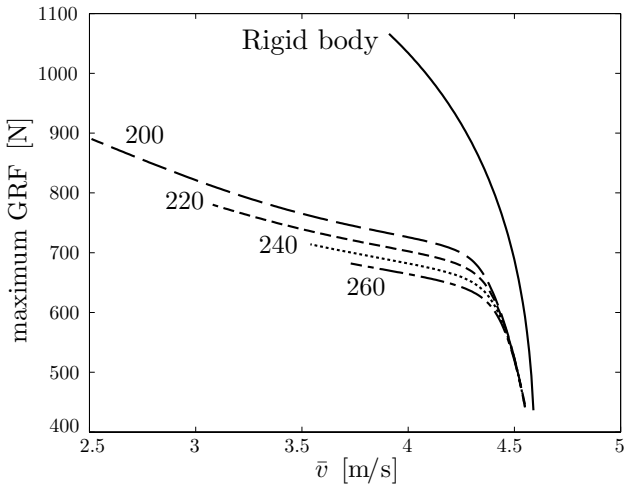

Fig. 4 Maximum ground reaction force for average speed of obtained gaits for various conditions of body stiffness. The *numbers* in this figure are the values of k_t

the rigid body model and the flexible body model with $k_t = 260$ Nm/rad, respectively. The results of other spring constants are qualitatively the same as that of Fig. 5b. At the apex height in the flexible body model, some energy is stored in a body joint spring and the gravitational potential

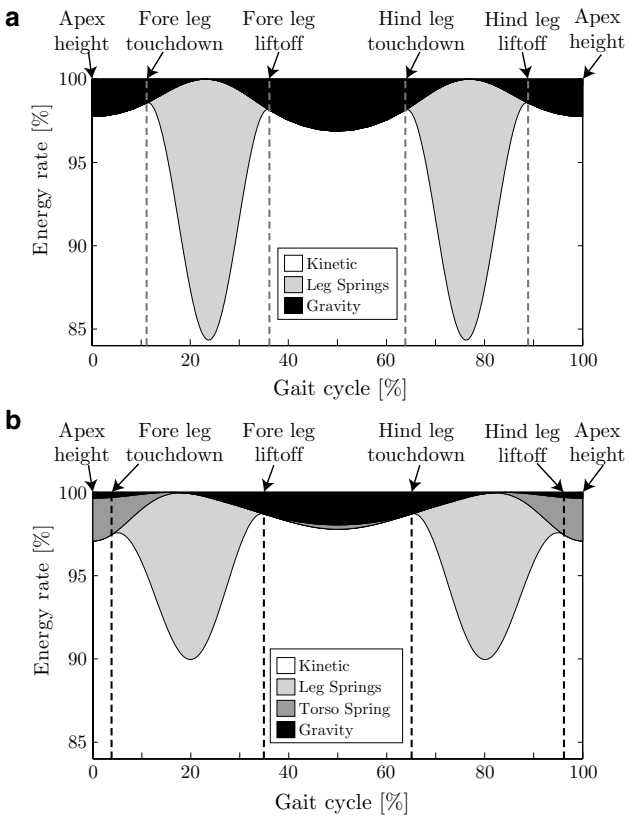

Fig. 5 Time profile of energy ratio at $\bar{v} = 4.5$ m/s. **a** The rigid body model and **b** the flexible body model with $k_t = 260$ Nm/rad

energy is smaller than that of the rigid body model. It suggests that the stored body spring energy reduces the gravitational potential energy and, as a result, the vertical motion and ground reaction force reduce.

6 Conclusion

In this paper, we investigated the effects of the flexibility of the body on bounding gait using two simple quadruped robot models. Simulation results showed that the maximum ground reaction force decreased by using a flexible body joint. This result is the most important contribution of this paper. It suggests that the flexibility of the body can reduce the burden of the robot during bounding gait. Therefore, to develop a quadruped robot that performs dynamic locomotion, it is important to have a proper stiffness in a body springy joint to reduce the foot loading of the robot.

In the present study, we fixed many parameters and only changed the body joint spring stiffness k_t and locomotion speed $\bar{v}$. In the future, we would like to search for periodic gaits using other parameters to investigate global properties of our models. In addition, for further understanding of the functional role of the body flexibility on gaits, we would

like to clarify the reason why the ground reaction force is decreased as the torso spring stiffness increased as shown in Fig. 4.

References

1. Raibert M (1986) Legged robots that balance. MIT Press, Cambridge
2. Poulakakis I, Smith J, Buehler M (2005) Modeling and experiments of untethered quadrupedal running with a bounding gait the Scout II robot. Int J Robot Res 24(4):239–256
3. Poulakakis I, Papadopoulos E, Buehler M (2006) On the stability of the passive dynamics of quadrupedal running with a bounding gait. Int J Robot Res 25(7):669–687
4. Remy C, Buffinton K, Siegwart R (2009) Stability analysis of passive dynamic walking of quadrupeds. Int J Robot Res 29(9):1173–1185
5. Nanua P, Waldron KJ (1995) Energy comparison between trot, bound, and gallop using a simple model. ASME J Biomech Eng 117(4):466–473
6. Alexander R (1988) Why mammals gallop. Am Zool 28(1):237–245
7. Culha U, Saranli U (2011) Quadrupedal bounding with an actuated spinal joint. In: Proceedings of IEEE international conference on robotics and automation, pp 1392–1397
8. Yamasaki R, Ambe Y, Aoi S, Matsuno F (2013) Quadrupedal bounding with spring-damper body joint. In: Proceedings of IEEE/RSJ international conference on intelligent robots and systems, pp 2345–2350
9. Cao Q, Poulakakis I (2013) Quadrupedal bounding with a segmented flexible torso: passive stability and feedback control. Bioinspir Biomemet 8(4):046007
10. Cao Q, Poulakakis I (2014) On the energetics of quadrupedal bounding with and without torso compliance. In: Proceedings of IEEE/RSJ international conference on intelligent robots and systems, pp 4901–4906
11. Farley C, Taylor R (1991) A mechanical trigger for the trot-gallop transition in horses. Science 253(5017):306–308